16A.6

THE WINTER 2010 FRONT/NIRSS IN-FLIGHT ICING DETECTION FIELD CAMPAIGN

David J. Serke* [a], John Hubbert [b], Scott Ellis [b], Andrew L. Reehorst [c], Patrick Kennedy [d], David Albo [a], Andrew Weekley [a] and Marcia K. Politovich [a]

[a] NCAR- National Center for Atmospheric Research
Research Applications Laboratory
Boulder, Colorado

[b] NCAR- National Center for Atmospheric Research
Earth Observing Laboratory
Boulder, Colorado

[c] NASA Glenn Research Center
Cleveland, Ohio

[d] Colorado State University
Department of Atmospheric Sciences
Fort Collins, Colorado

1. INTRODUCTION

When air below the freezing point of 0°C becomes supersaturated with respect to water and ice, ice crystals begin to grow on freezing nuclei such as mineral dust, aerosols, other pollution particles or existing ice crystals by the process of diffusion (Rogers and Yau, 1988). In the absence of significant populations of such freezing nuclei, liquid water drops begin to condense out of the air from the water vapor. These drops are liquid that exist below freezing – or supercooled liquid water (SLW). In-flight icing occurs when an aircraft impacts with these SLW drops, which instantly freeze to the airframe. The resulting ice accretion builds up on the leading edges of the airframe's control surfaces. Supercooled large drops (SLD), defined as drops larger than 50 μm, can accrete beyond the leading edges of the airframe where any existing ice mitigation technology such as boots and warmed surfaces would have no effect. Ice accretion while in flight acts to increase drag and reduce the aerodynamic lift generated by a vehicle's control surfaces. Significant ice buildup can change an aircraft's flight characteristics enough to be a significant safety hazard and has been recognized as a contributing factor to many crashes with resulting loss of life.

This study will focus on methods to utilize two ground-based remote sensing platforms with the purpose of providing accurate and timely warnings on the presence of in-flight icing hazard. One such platform is the national network of Doppler radars, known as NEXRADs (NEXt-generation RADars, or WSR-88Ds). These 11 cm wavelength S-band radars are designed to detect the presence of precipitation-sized particles, such as snow, rain and hail. However, the cross-sectional dimension of SLW drops are often several factors of ten smaller than these precipitation particle categories. One well known attribute of millimeter wavelength radars are that they tend to backscatter power from a target proportional to the sixth power of the target's diameter (Bringi and Chandrasekar, 2001). For example, this means that for a radar viewing a sample volume which contained one large snowflake and a million much smaller SLW drops, the returned power to the radar receiver would be dominated by the single large snowflake. This fact limits the radar's capacity to detect these small SLW drops, which can make big problems for aircraft.

Existing NEXRADs transmit and receive only horizontal polarization, and thus measure reflectivity (REFL), radial velocity and spectrum width. Previous research with the singularly polarized 4-dimensional national NEXRAD mosaic (Serke et al., 2008) found that mixed phase conditions were virtually impossible to determine directly, however, data suggested that certain spatial relations might exist between SLW and the location and intensity of the radar reflectivity field. In cases with icing research flights, areas with reflectivity corresponding to 'all snow' had reflectivity generally above 20 dBZ with low spatial standard deviations. Higher SLW values existed in areas of reflectivity generally below zero, and in reflectivity gaps where the radar return was below the minimum detected by the radar at a given range. This work suggested that areas

---

*Corresponding author address: David J. Serke, National Center for Atmospheric Research, PO Box 3000, Boulder, CO 80307, dserke@ucar.edu

lacking SLW could possibly be identified with just radar reflectivity. Identifying cloudy and non-cloudy airspace that does not contain an icing hazard is an important step in qualifying the total airspace volume.

Presently, NOAA has begun the process of upgrading the national network of NEXRADs so that they are capable of transmitting and receiving both vertical and horizontal radiation – known as 'dual polarization'. This project is scheduled to be completed within two years. While polarized NEXRAD data are currently unavailable beyond the prototype KOUN radar in Norman, Oklahoma and a few other recently upgraded sites, two research radars exist along the Front Range of Colorado which have very similar characteristics to polarized NEXRADs. Dual-polarized radars collect additional information that can give researchers insight as to the mean particle shape, size, phase (liquid or solid), bulk density and preferred particle orientation in a given sampled volume. Polarized radars collect differential reflectivity (Zdr), correlation coefficient (ρ_{HV}), linear depolarization ratio and specific differential phase. Differential reflectivity is the ratio of horizontal co-polar received power to the vertical co-polar return. One way to interpret this field is a power-weighted mean axis ratio of the particles in the volume. Small liquid and cloud drops are nearly round, so Zdr values are near zero and small reflectivity. Larger drops become oblate as they fall and thus Zdr between 0.3 and 2.0 dB. Oriented ice crystals also have Zdrs that are positive and large. ρ_{HV} is the correlation between horizontal and vertical co-polar received returns. Wet or tumbling particles and mixed phase conditions result in de-correlation in polarizations so that ρ_{HV} values are typically below 0.92. Homogeneous rain or ice result in ρ_{HV} values above 0.95. Plummer et al., (2010) explored some of these polarized moment relations in regards to in-flight icing situations.

To further test the information content of the polarized moment data with respect to icing, the authors arranged a field campaign where radar data was collected during the winter of 2010/2011 during in-flight icing cases. One goal of this field campaign was to test the viability of an in-flight 'Icing Hazard Level' (IHL) algorithm (Smalley et al., 2009) for the National Weather Service's network of 150 soon-to-be polarized NEXRADs. The current incarnation of the IHL algorithm is a hybrid of several existing precipitation identification algorithms. For this study, testing was accomplished by exploring the vertical profiles of moment fields from the research radars at times of known icing and known absence of icing. In the absence of expensive icing flights flown with specially outfitted research aircraft, verification and validation of the presence of in-flight icing were provided by pilot reports and by NASA's Icing Remote Sensing System (NIRSS).

No single instrument has yet been developed which can unambiguously detect in-flight icing conditions. For this reason, combinations of sensors have been under development for some time to detect in-flight icing (Politovich et al, 1995, Bernstein et al., 2005). NIRSS is a prototype ground-based remote sensing platform used to detect in-flight icing that has been under development by NASA and NCAR since 2003 (Reehorst et al., 2006). The mandate of the NIRSS program is to detect in-flight icing in the near-airport environment with existing, relatively inexpensive technologies. A recent study found that NIRSS detects the absence, presence and severity of in-flight icing at least as well as the FAA's current operational system to detect icing (Johnston et al., 2011). The second goal of this field campaign was to test and improve the prototype NIRSS.

2. Field Campaign

2.1 Overview

To address the goals of this study, the authors brought the mobile NIRSS from its traditional home at NASA Glenn Research Center in Cleveland, Ohio, to the Front Range of Colorado for the period of December 2010 to June 2011. It was deployed at the NOAA-owned Platteville site due to the site's proximity to the CSU-CHILL radar, the NSF S-Pol radar as well being located under the flight path of commercial aircraft arriving and departing from Denver's International Airport (DIA). The positions of the respective instrumentation for this field campaign are shown in Fig. 1. Proximity to DIA provided the best chance of being

***Figure 1**. – Map of the Front Range of Colorado, showing the location of instrumentation platforms and distances to NIRSS.*

close to the greatest number of voluntary pilot reports of in-flight icing that might occur over the deployment period. Also, twice daily meteorological balloon soundings and surface condition reporting from DIA could be utilized for case study analyses. Platteville is also home to NOAA's 449 MHz acoustic atmospheric wind profiler. Each instrument platform or source of comparison data are described in detail in the following paragraphs.

2.2 Instrumentation

2.2.1 Polarized Research Radars

The Front Range of Colorado was chosen for this experiment because it is home to two of the world's premier polarized S-band research radars – Colorado State University's CHILL radar (CSU-CHILL) and NSF's S-Pol radar. CHILL (Fig. 2, Brunkow et al., 2000) is located 7 km northeast of Greeley, CO. S-Pol (Fig. 3) is located several kilometers southeast of Boulder, CO. Relevant characteristics for each of the radars are shown in Table 1, respectively. During icing cases,

***Figure** 2. The CSU-CHILL research radar near Greeley, CO.*

***Figure 3**. – The NSF S-POL research radar near Boulder, CO.*

***Table 1**. – Characteristics of CSU's CHILL and NSF's S-Pol Radars.*

		CSU-CHILL	NCAR-SPOL
Antenna			
	Type	Fully steerable, dual offset feed	Fully steerable, parabolic
	Size	8.5 m	8.5 m
	Feed	Scalar horn	Center
	Half-power beamwidth	1.0 deg	0.91 deg
	Gain	45 dB	44.5 dB
	Polarization	Horiz. or vert.	Horiz. or vert.
	Max scan rate	18 deg, each axis	18 deg, each axis
	Scan type	PPI,RHI, sector	PPI, RHI, sector
Transmitter			
	Type	Klystron, FPS-18	Klystron, ASR-9
	Wavelength	11 cm	11 cm
	Peak power	~1 Mw	> 1 Mw
	Pulse width	0.1~ 1.0 μs	0.3~ 1.4 μs
	PRT	800~2500 μs	800~2500 μs
	Max. unamb. range	375 km	375 km
Receiver			
	Noise figure	3.4 dB	2.9 dB
	Transfer func.	Linear	Linear
	Dynamic range	> 85 dB	90 dB
	Min. detect.	-112 dBm	-52 dBZ @ 1km -15 dBZ @ 50 km
	Pol. signal	Alternating or simultaneous	Alternating or simultaneous

each of the two radars executed a scan routine which included several range versus height scans in the azimuthal direction of Platteville, followed by a series of stacked 360° scans which varied from 0.5 to 11 degrees in elevation. The stacked elevation scan volume was chosen to be similar to a typical NEXRAD storm-mode scan routine.

2.2.2 NIRSS

NIRSS consists of a vertically pointing Doppler Ka-band radar, a multichannel microwave radiometer and a laser ceilometer (Fig. 4, Reehorst et al., 2006). The system employs a multi-channel radiometer built by Radiometrics Corporation, which passively collects incoming microwave radiation at a number of channels in the K and V-bands of the electromagnetic spectrum (Solheim et al., 1998). The K-band lies within an atmospheric window and thus variations at specific frequencies within the band are due to variations in the amount of liquid and gaseous water. Different amounts of gaseous and liquid phase water cause the amount of microwave radiation received by the radiometer at frequencies frequencies within the K-band to respond differently. Algorithms used within the radiometer's software compare the integrated liquid water (ILW) and integrated water vapor (IWV) of large historical archives of station sounding data to the inverted radiometric brightness temperatures from the instrument in order to arrive at ILW and IWV values for a given realtime radiometer profile. The instrument's V-band channels are on the shoulder of a major oxygen absorption feature, so that progressively varying frequencies from the peak of the absorption feature yields information on the atmospheric temperature further from the radiometer in range. This allows for the derivation of an atmospheric temperature profile.

***Figure 4**. – NIRSS components stationed at Platteville, CO.*

All input data streams are ingested into a 'fusion' machine and software is used to combine the instrument fields into an in-flight icing product. The height range of the 0 and -20° Celsius isotherms are targeted as the area where in-flight icing could exist. The vertical extent of cloud boundaries are provided by the ceilometer and Ka-band cloud radar. If cloud exists within the height range where icing temperatures exist, any liquid sensed by the radiometer is then distributed vertically with fuzzy logic based on previous experience with years of research flights in icing conditions (Reehorst et al., 2005).

2.2.3 Pilot Reports

Pilot Reports (PIREPs) are voluntary reports made by commercial airline pilots of the time and location of meteorological conditions that their flight has encountered. In-flight icing is one of many possible conditions that can be reported. The existence of icing can be reported as 'no icing exists' or 'icing exists' with a severity of 'trace', 'light', 'moderate', 'severe' or 'heavy' or 'severe'. The authors converted these qualitative conventions to a 0-8 scale for ease of comparison. Over the course of the field campaign, over 350 icing PIREPs were reported within 50 km of NIRSS, 60 of which were within 25 km.

2.2.4 Precipitation and temperature observations

Surface observations of present weather and twice daily balloon-sondes from Denver International Airport are incorporated into the case study analyses in the following section. Starting in mid-February, a Parsivel distrometer (Loffler-Mang and Joss, 2000) was located with NIRSS in order to quantify the time, size and number of precipitation particles. The importance of having precipitation data is that it can often give information about synoptic weather features and processes that are occurring in the atmospheric column.

3. Case Studies

The method that was chosen to analyze the archive of in-flight icing cases collected during the 2010/2011 field campaign was to collect radar moment profiles at the exact times of interest based on the NIRSS ILW and icing hazard severity fields. Since it is difficult to discern the presence of mixed-phase conditions from just single profiles of S-band radar data, each time period of interest will portray all of the profiles within 250 meters of the NIRSS location. This corresponds to the 9 geographically closest profiles from a given range versus height volume scan. This many profiles on a single plot becomes very busy, but important trends exist in the horizontal as well as the vertical standard deviations of moment data that will

become evident through this plotting and analysis method. Similar work to this was done with horizontal standard deviations of NEXRAD reflectivity in a paper by Ikeda et al. (2009).

Over 350 icing PIREPs were collected within 50 km of the Platteville site during the campaign, but it became increasingly obvious that the scale of SLW features within the study area and the known inaccuracies of the time and location of PIREPs would not allow accurate comparison to our collected PIREP database. For this reason and the fact that the NIRSS testbed has proven itself significantly accurate when compared to past icing research flights (Reehorst et al., 2005), this study relied on the NIRSS ILW and icing hazard product to compare to the S-band moment data profiles as opposed to PIREPs. PIREP times and icing severities were only used as an indicator of the presence of in-flight conditions within the study area. Three icing case studies follow.

3.1 December 30th through 31st, 2010

On December 30th, 2010, a strong Artic cold front combined with an upper-level low pressure system over Colorado to bring upsloping winds from the north

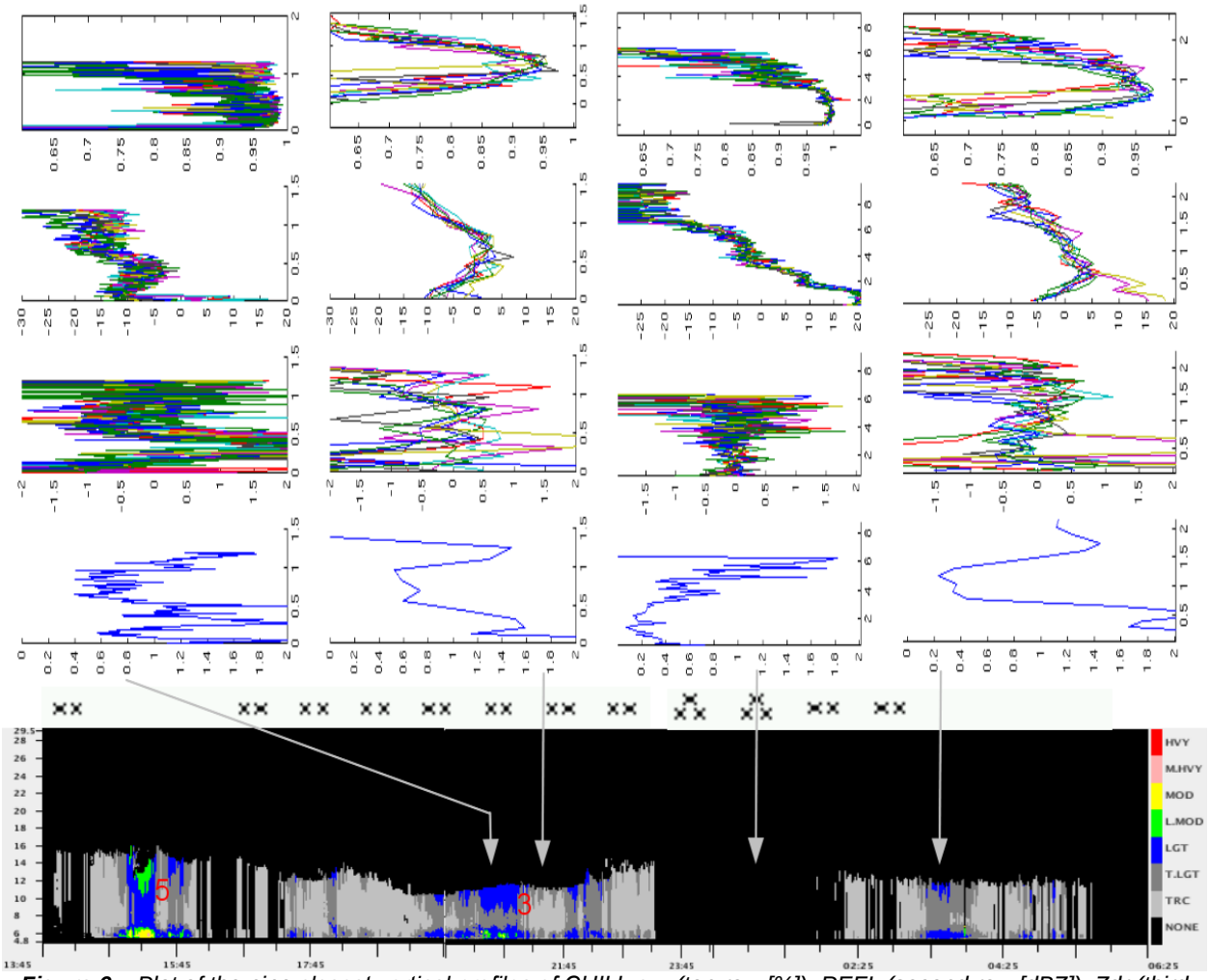

Figure 6 *– Plot of the nine closest vertical profiles of CHILL ρ_{HV} (top row,[%]), REFL (second row,[dBZ]), Zdr (third row,[dB]) and horizontal standard deviation of Zdr (fourth row)to Platteville, CO on December 30-31st 2010 at the times shown by the grey arrows on the time/height plot of NIRSS icing hazard (bottom row, color scale). The time, height and severity of icing PIREPs are shown in red numerals. A time series of observed weather from DIA is also shown ('xx' and 'xxx' symbols represent snow rates).*

and east over Platteville (not shown). Since terrain slopes gently upwards toward the mountains from east to west along the Front Range of Colorado, any wind flow with a significant easterly component effectively lifts an air mass and is thus called 'upslope'. This is one of the main forcing mechanisms for wintertime in-flight icing events in this region. The system brought periods of moderate snow and no associated icing PIREPs, interspersed with periods of no snow and moderate icing PIREPs. Fifteen icing PIREPs were reported within 50 km of Platteville during this case. Surface temperatures were below freezing for the entire case study period (not shown). NIRSS's icing hazard algorithm detected these periodic icing times well (Fig. 6, bottom row). CHILL began operations at 17:40 UTC and continued through the end of the icing case on December 31st. At 20:26 UTC, NIRSS detected moderate icing. CHILL moment data from this time are plotted in the first column of Fig. 6 as 9 different colored profiles for each moment field. CHILL detected only REFLs below 0 dbZ, with a discrete second layer of even lower REFL above 0.6 km AGL. Values for ρ_{HV} were above 0.9, but with significant variability, especially in the upper cloud layer. Zdr in the upper layer was centered near 0.0 dB and had the lowest horizontal variability. One hour later at 21:20 UTC, NIRSS detected a rapid decrease in icing but still enough liquid for a 'trace' hazard designation. CHILL saw an overall increase in mean REFL through the column and a more uniform vertical distribution of REFL from the previous time's two discrete layers (Fig. 6, second column). There was somewhat more variability in the 9 Zdr profiles nearest to Platteville at this time compared to the previous time. An increase in the snowfall rate was observed at around 1:00 UTC on December 31st, and NIRSS detected no liquid and no icing hazard around this period. This is consistent with the theory of a uniform ice crystal population in the sampled profile effectively scavenging out any available liquid. CHILL moment profiles at this time (Fig. 6, third column) show REFLs above 0 dBZ up to 3 km AGL, which correlates to returns from the moderate snowfall. ρ_{HV} was close to 1.0, indicating a uniformly shaped particle population. Zdr was close to 0 dB, which in this case is probably indicative of tumbling ice crystals. Horizontal variation of Zdr in this layer was also low. At 3:30 UTC, no precipitation was reported at the surface and NIRSS was indicating significant icing. REFLs were mostly below 5 dBZ, and Zdr was fairly variable except for in the cloud section centered at 1km AGL (Fig. 6, fourth column). Here, Zdr was centered on 0 dB and had a very low horizontal standard deviation.

3.2 March 7th, 2011

On March 7th, 2011, a slow-moving surface low pressure system over north-central Colorado acted to create an upslope wind component along the Front Range of Colorado for a full 24-h period beginning at roughly 6:00 UTC. The surface precipitation was observed at DIA (Fig. 7, bottom) and by the Parsivel distrometer located at Platteville (data not shown) as periods of light showers and transitioned to haze, fog and freezing drizzle by 9:00 UTC. A total of 17 icing PIREPs were reported within 50 km of Platteville during this case. Surface temperatures were below freezing for the entire case study period (not shown). NIRSS detected the start and stop times and vertical extent of icing very well when compared to PIREPs. CHILL began operations at 17:00 UTC and continued through the end of the day. At 17:30 UTC, NIRSS detected light to light/moderate icing hazard values. Since this case was uniformly stratiform in nature all along the Northern Front Range for the duration of the case, and since the radar signal disappeared below the minimum detectable by the radar at ranges greater than 10 km distance, analysis relied on the radar moment profiles at 5 km distance in the direction of Platteville instead of the 30 km distance that Platteville is from CHILL. CHILL (Fig. 7, first column) detected a very weak signal for this case due to the uniform liquid after 9:00 UTC. REFL at or below -20 dbZ existed through the cloud depth up to the tops at 0.8 km. ρ_{HV} values were extremely variable and never got above 0.90. Zdr values were extremely variable in this low return scenario. Previous research shows that Zdr values do not have any significant information content at these low signal-to-noise ratios. At time 21:45 (Fig. 7, second column) a light to moderate icing PIREP was recorded at 8,000 ft AGL. The radar profiles were much the same as during the previous time, with a shallow layer of very low REFLs and ρ_{HV} values significantly below 0.90.

3.3 May 18th, 2011

On May18th, 2011, A fast moving low-pressure system travelled southeastward along the Front Range of Colorado. Early in the day, the system was centered south of Denver. By 6:00 UTC the system had tracked towards the Oklahoma-Texas panhandle with an inverted trough extended from the center of the low pressure along the far eastern plains of Colorado. After 15:00 UTC pressure gradually dropped as a secondary inverted trough formed along the Front Range. At 18:00 UTC, the surface chart and infrared satellite image (not shown) showed an extensive area of cloud cover forming over the Front Range. After 18:00 UTC, convection began to form in the higher terrain of the Front Range and moved off the mountains onto the Eastern Plains. The DIA meteogram shows thunderstorms in the area from 19:00 UTC onward for the remainder of the day (Fig. 8, symbols). The temperature sounding at DIA at 00:00 UTC on May 19th showed the freezing level at about 1 km altitude AGL

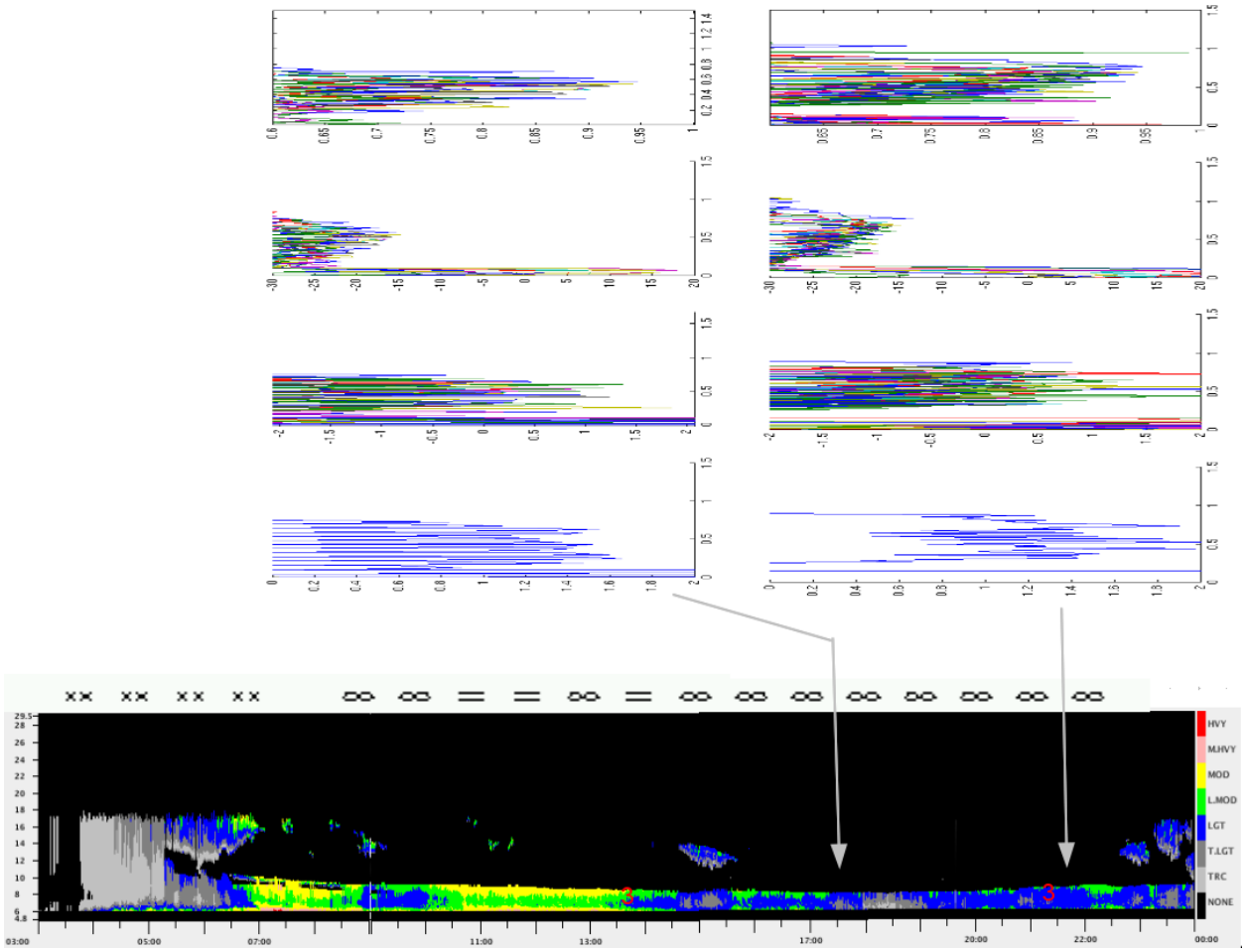

Figure 7 *– Plot of the nine closest vertical profiles of CHILL ρ_{HV} (top row,[%]), REFL (second row,[dBZ]), Zdr (third row,[dB]) and horizontal standard deviation of Zdr (fourth row)to Platteville, CO on March 7th 2011 at the times shown by the grey arrows on the time/height plot of NIRSS icing hazard (bottom row, color scale). The time, height and severity of icing PIREPs are shown in red numerals. A time series of observed present weather from DIA is also shown (symbols).*

(not shown). CHILL was operating from 19:50 UTC through the end of the day. Four 'light' to 'moderate' icing PIREPs were reported within 30 km of Platteville between 18:00 and 20:00 UTC on this date (Fig. 8, bottom row, red numbers). These PIREPs reported icing between 10,000 and 20,000 feet AGL (between 3.1 and 6.1 km AGL). The NIRSS hazard output had icing between 10,000 and 20,000 feet AGL at the Platteville site, with severity values ranging up to 'moderate'. At 19:54 UTC, no precipitation was measured at the surface by the distrometer. At 19:54 UTC (Fig. 8, upper left), ρ_{HV} values were uniformly near 1.0 up to 6 km AGL and were reduced and variable above that level. REFL were between 0 and 10 dBZ up to 6 km AGL. Zdr was slightly positive in the cloud layer up to 6km and was near zero and highly variable horizontally above 6 km altitude. In the cloud layer above the 1 km melting level, the horizontal standard deviation of Zdr was relatively low. At the melting level and below, Zdr was again relatively large. By 21:54 UTC, the distrometer at Platteville was detecting rain associated with the nearby shower and thunderstorm activity. At 21:54 UTC (Fig. 8, upper right), a relative minima in the ρ_{HV} signal is evident at 1 km associated with the pronounced melting level. The ρ_{HV} signal above 5.5 km also becomes more variable and is generally below 0.93. REFL values above 5.5 km are below 0 dBZ and exhibit significant variability horizontally (consistent with Ikeda et. al 2009 findings). The largest vertical gradients in REFL occur right at 5.5 km and at the 1 km freezing levels. Zdr above 5.5 km is highly variable, but centered at about 0 dB. Zdr below 5.5 km

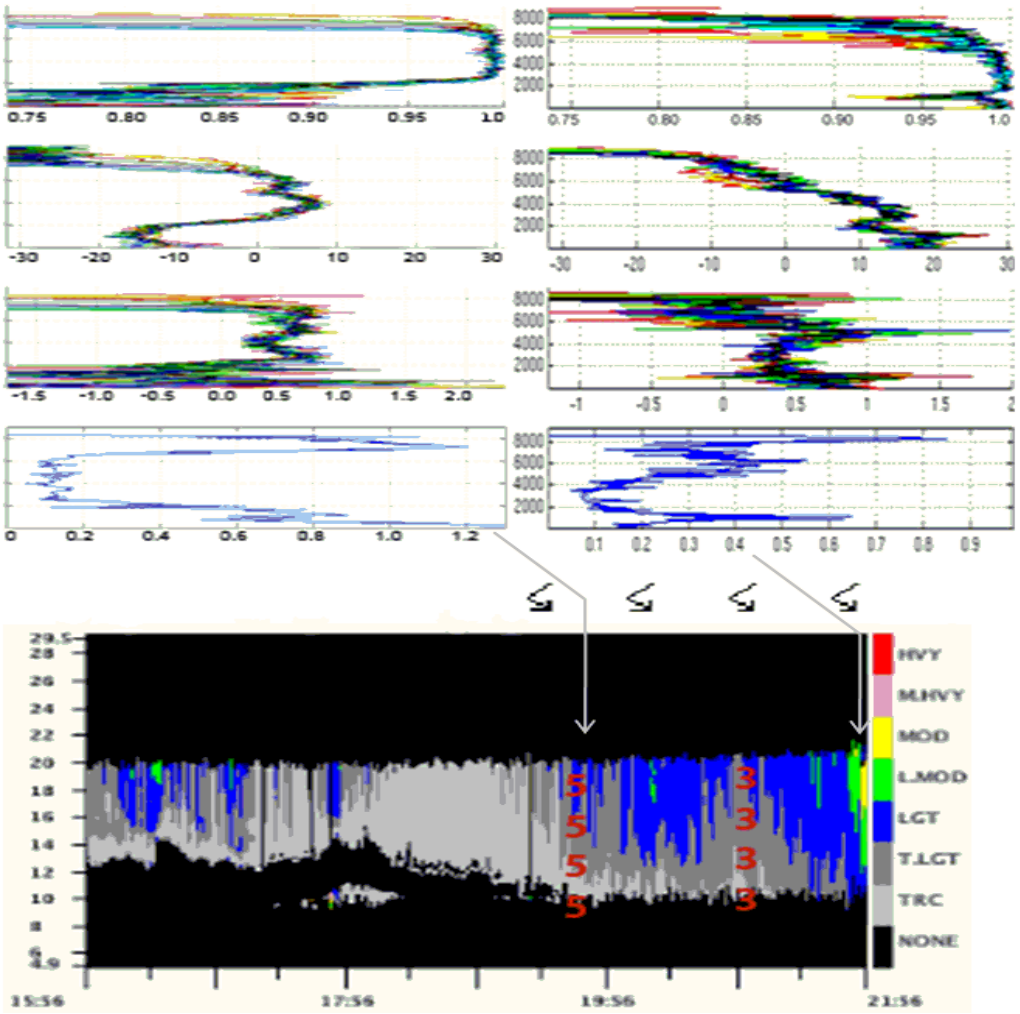

Figure 8 *– Plot of the nine closest vertical profiles of CHILL ρ_{HV} (top row,[%]), REFL (second row,[dBZ]), Zdr (third row,[dB]) and horizontal standard deviation of Zdr (fourth row)to Platteville, CO on May 18th 2011 at the times shown by the grey arrows on the time/height plot of NIRSS icing hazard (bottom row, color scale). The time, height and severity of icing PIREPs are shown in red numerals. A time series of observed present weather from DIA is also shown (symbols).*

are generally slightly greater than 0 dB. Relative maxima in Zdr occur near 5.5 km and near the melting level at 1 km altitude. The horizontal standard deviation of Zdr is at a relatively elevated level above 5.5 km, and also has a relative maxima at the melting level.

SUMMARY

During the winter of 2010/2011, NIRSS was positioned at Platteville, CO, between CSU's CHILL and NSF's S-Pol polarized research radars and underneath the flight-path of aircraft going to and from Denver's International Airport. The purpose of this field campaign was to further test the prototype NIRSS system as well as provide in-flight icing verification data to compare to the moment data from the polarized research radars. This work was conducted to determine the overall feasibility of using polarized precipitation radar fields to construct an 'Icing Hazard Level' algorithm for the soon-to-be upgraded national network of S-band NEXRADs.

The authors have analyzed multiple polarized radar moment profiles within 0.5 km of the vertically staring NIRSS during periods of no icing, low and significant icing for all icing events during the winter field

campaign and have observed several signatures in the moment profiles that could be utilized. A lack of icing has been seen to be characterized by REFLs generally above 15 dBZ and ρ_{HV} above 0.92. The relatively large REFLs are representative of ice crystal populations that have had time to scavenge out any available liquid, and elevated ρ_{HV} is indicative of a uniformly shaped particle population. In these instances, Zdrs are most likely to be near 0 dB due to the tumbling nature of the relatively large regular or irregular ice shapes. Horizontal standard deviations of all moment data in these 'all snow' cases are generally relatively small, as these snow cases have generally had time to develop horizontally and tend not to be cellular in nature. In mature 'all snow' cases, REFL tended to increase, Zdr tended to focus more toward 0 dB, and horizontal standard deviations of Zdr tended to decrease from the top to the bottom of the respective profiles. The most difficult positive icing scenarios for these polarized precipitation radars to detect appear to be homogeneous small or large drop icing. The signals returned from these SLW particles are very weak since the sizes of the SLW are generally smaller than typical precipitation particles. These cases often manifest as a 'donut-shaped' pattern close-in around the radar in fixed elevation scans. REFL can be from -15 dBZ down to the minimum detectable signal at the given range from the radar. Zdrs and other cross-polar fields are often meaningless at these extremely low signal-to-noise ratios. ρ_{HV} values in these cases have been seen to be highly variable but well below the 0.90-0.92 range seen in typical 'all snow' scenarios. These cases can be properly identified as homogeneous SLW cases by recognizing that the majority of these events are stratiform in nature and can thus be extrapolated up through the upper cloud limits at all locations between adjacent radars that exhibit similar return patterns at coincident times.

Mixed-phase cases have historically been the most important and most difficult problems for determining the existence of in-flight icing. Radar return is governed by the mean particle diameter to the 6^{th} power, ensuring that the largest particles dominate. In this study, it was shown that several general patterns may exist in the temporally evolving vertical and horizontal radar moment fields that could be used to detect the presence of liquid in an otherwise glaciated cloud. One pattern for times of significant ILW, as viewed by NIRSS, was REFLs below 5 dBZ coexisting with Zdrs near 0dB that also had low horizontal standard deviations in Zdr. This indicates the presence of not many and/or not large ice crystals due to the relatively low REFLs. Zdrs near zero were consistent with cross-polar returns that were nearly identical – possibly due to a mean spherical shape as in liquid. The elevated layers of relative minimum horizontal standard deviation in Zdr are a pattern attributable to water. Previous studies (such as Ikeda et al., 2009) have shown the 'smoothness' in Zdr coincided with liquid, whereas more highly variable horizontal values were consistent with homogeneous ice phase. In the third case discussed in this work, REFLs were between the somewhat arbitrary 5 dDZ threshold, below which defined 'homogeneous liquid' and above 15 dBZ which was used to define 'all snow' cases. ZDRs were seen to spike from +1 to +4 dB from a period where no ILW was sensed by NIRSS to a subsequent period when significant ILW was sensed by NIRSS in a narrow elevated layer of the cloud. These elevated Zdr features can be interpreted as rapid growth in horizontally oriented ice crystals due to scavenging of coexistent SLW. Such features were very highly time-dependent and were associated with much more cellular storm features than seen in the more stratiform 'all snow' or 'homogeneous liquid' cases. This was evidenced by the maximum in horizontal standard deviation of Zdrs just below the height of the SLW layer, which corresponds to microscale spatial variability in the location of the oriented crystals falling out below the SLW layer as a developing snow shower. These relations appear to be valid over a large range of in-flight icing scenarios, such as stratiform small-drop SLW cases that are subfreezing through the whole atmospheric column, to weakly convective springtime stratiform cases with elevated melting layers.

Future work includes comparison of S-Pol and CHILL data during these times of interest and building an initial codebase to attempt to automatically quantify icing with NIRSS and polarized S-band radars in the Icing Hazard Level algorithm. Some early results of this work with these field campaign data sets are shown in poster number 204 at this conference. Another future direction would expand this study's findings beyond case studies to a statistical analysis of all NIRSS ka-band and S-band polarimetric profiles at icing and non-icing times to further determine what generalizations could be made. NIRSS project tasking involves further testing and integration of the NASA Narrow-beam Multi-channel Microwave Radiometer (NNMMR) into NIRSS in order to derive a volumetric icing hazard for the near-airport environment. The NNMMSR scan drive motor will be upgraded with new hardware so that the scan routine can be made to be synchronized with a typical NEXRAD scan routine. This would allow a future NIRSS version with an integrated NNMMSR to provide synergistic in-flight icing detection with polarized NEXRAD data, as was explored in this work.

ACKNOWLEDGEMENTS

This research is supported by the NASA Aviation Safety Program, under the Atmospheric Environment Safety Technologies (AEST) project. The views expressed are those of the authors and do not

necessarily represent the official policy or position of the NASA. The authors would like to thank and acknowledge the National Oceanographic and Atmospheric Association for allowing us to locate our instrument platform at their Platteville Atmospheric Observatory site. The authors would also like to thank and acknowledge the Colorado University Space Physics Group led by Dr. Scott Palo for allowing us the use of their internet connection at Platteville.

REFERENCES

Bernstein, B., McDonough, F., Politovich, M., Brown, B., Ratvasky, T., Miller, D., Wolff, C., and Cunning, G., "Current Icing Potential: algorithm description and comparison to aircraft observations", *J. Appl. Meteor*., **44**, pp. 969-986, 2005.

Bringi, V. and Chandrasekar, V., "Polarimetric Doppler Weather Radar – Principles and applications.", *Cambridge University Press*, 656 pp., 2001.

Brunkow, D., Bringi, V. N., Kennedy, P, Rutledge, S., Chandrasekar, V., Mueller, E. and Bowie, R., "A description of the CSU–CHILL National Radar Facility", *J. Atmos. Ocean. Tech*, **17**, Issue 12, pp. 1596-1608, 2000.

Ikeda, K., Rasmussen, R., Brandes, E. and McDonough, F., "Freezing Drizzle Detection with WSR-88D Radars", *J. Appl. Meteor. Climatol.*, **48**, 41–60, 2009. [doi: 10.1175/2008JAMC1939.1]

Johnston, C., Serke, D., Adriaansen, D., Reehorst, A., Politovich, M.,Wolff, C. and McDonough, F., "Comparison of in-situ, model and ground based in-flight icing severity", *AMS Conference Preprint*, Seattle, WA, Jan 24-27, 2011.

Loffler-Mang, M., and Joss, J., "An optical disdrometer for measuring size and velocity of hydrometeors", *J. Atmos. Ocean. Tech*., **17**, 130-139, 2000.

Plummer, D., Göke, S., Rauber, R. and Di Girolamo, L.,"Discrimination of mixed- versus ice-phase clouds using dual-polarization radar with application to detection of aircraft icing regions", *J. of Appl. Meteor. and Clim.*, **49**, Issue 5, pp. 920-936, 2010. [doi: 10.1175/2009JAMC2267.1]

Politovich, M.K., B.B. Stankov and B.E. Martner, "Determination of liquid water altitudes using combined remote sensors", *J. Appl. Meteor*., **34**, pp. 2060—2075, 1995.

Reehorst, A.L., Brinker, D.J., Ratvasky, T.P., "NASA Icing Remote Sensing System: comparisons from AIRS–II," NASA/TM—2005-213592, 2005.

Reehorst, A., Politovich, M., Zednik, S., Isaac, G. and Cober, S., "Progress in the development of practical remote detection of icing conditions", *NASA/TM 2006-214242*, NASA, 2006.

Rogers, R., and Yau, M., "A Short Course in Cloud Physics", Elsevier Science, Oxford, UK, 1988.

Serke, D. J., F. McDonough and M. Politovich, "Analysis of 3-D NEXRAD Mosaic reflectivity data collocated with research aircraft and satellite data: implications on in-flight icing". *13th Conference on Aviation, Range and Aerospace Meteorology Preprint*, New Orleans, LA, Jan 20-25, 2008.

Smalley, D., Bennett, B., Hallowell, R., Donovan, M., and Williams, E., "Development of dual polarization aviation weather products for the FAA", *AMS Conference Preprint*, 2009.

Solheim, F., Godwin, J., Westwater, E., Han, Y., Keihm, S., Marsh, K., and Ware, R., "Radiometric profiling of temperature, water vapor and cloud liquid water using various inversion methods", *Radio Sci.*, **33**, pp. 393-404, 1998.